12th Hel.A.S Conference
Thessaloniki, 28 June- 2 July, 2015
CONTRIBUTED POSTER

Spectral signatures of compact sources in the inverse Compton catastrophe limit

M. Petropoulou[1], *T. Piran*[2], *S. Boula*[3], *A. Mastichiadis*[3]
[1]Department of Physics and Astronomy, Purdue University, West Lafayette, IN 47907, USA
[2]Racah Institute of Physics, The Hebrew University, Jerusalem 91904, Israel
[3]Department of Physics, University of Athens

Abstract: The inverse Compton catastrophe is defined as a dramatic rise in the luminosity of inverse Compton scattered photons (e.g. [1], [2], [3]). It is described by a non-linear loop of radiative processes that sets in for high values of the electron compactness, and is responsible for the efficient transfer of energy from electrons to photons, predominantly through inverse Compton scatterings. We search for the physical conditions that drive a non-thermal emitting source to the inverse Compton catastrophe regime, and then study the emergent multi-wavelength (MW) photon spectra. We find that the escaping radiation from a source that is driven deep in the Compton catastrophe regime bears some unique features. The MW photon spectrum is a broken power law with a (comoving) break energy of $\sim m_{\rm e}c^2$ due to the onset of the Klein-Nishina suppression. While the spectral index above the break energy depends on the power-law index of electrons at injection, this does not apply to the spectral index below the break, which depends logarithmically on the electron and magnetic compactnesses and typically lies in the range 0.5-0.9.

1. Model Assumptions

We assume that mono-energetic relativistic electrons with Lorentz factor γ_0 are injected with a rate Q_0 in a spherical source of radius $r_{\rm b}$ that is moving with Lorentz factor Γ. These electrons lose energy through synchrotron radiation on an embedded magnetic field of strength B as well as through inverse Compton scattering on the internally produced synchrotron photons (Synchrotron Self-Compton – SSC) and on external photons (external Compton – EC). In addition the characteristic timescale of electron escape is $t_{\rm e,esc}=r_{\rm b}/c$, that is also equal to the typical timescale for adiabatic losses. We approximate the emissivity of synchrotron and inverse Compton scattering by a δ-function centered at (dimensionless) photon energies $x_{\rm syn}=b\gamma_0^2$ and $x_{\rm ssc,i}=(4/3)^i b\gamma_0^{2(i+1)}$, respectively. $x_{\rm ssc,i}$ is the energy of a photon that has been Compton up-scattered i-times, $b=B/B_{\rm cr}$ with $B_{\rm cr}=4.4\times10^{13}$ G. The highest order of up-scattered photons in the Thomson regime is $N_{\rm T}=\left[\frac{\log(1/b\gamma_0)}{\log\left(4\gamma_0^2/3\right)}\right]$. Even higher photon generations are suppressed due to the Klein-Nishina cutoff. The kinetic equation for electrons is described by $\frac{\partial n_{\rm e}(\gamma,t)}{\partial t}+\frac{n_{\rm e}(\gamma,t)}{t_{\rm e,esc}}=Q_e(\gamma,t)+\mathcal{L}_e(\gamma,t)$, where $n_{\rm e}$ is the differential electron density and Q_e, $\mathcal{L}_e$ are the injection and energy loss operators for electrons, respectively. These are defined as $Q_{\rm e}=Q_0\delta(\gamma-\gamma_0)H(t)$, $\mathcal{L}_e=\frac{4}{3}\frac{\sigma_{\rm T}c}{m_ec^2}\frac{\partial}{\partial\gamma}\left[\gamma^2 n_{\rm e}(\gamma,t)u_{\rm tot}\right]$, where $H(x)$ is the Heaviside function and $u_{\rm tot}$ is the total energy density. This is given by $u_{\rm tot}=u_{\rm B}+u_{\rm ex}+u_{\rm syn}+\sum_{i=1}^{N_{\rm T}-1}u_{\rm ssc,i}$. Some useful definitions follow:

- the compactness of a field that is a dimensionless measure of its energy density $\ell_{\rm j}=\frac{\sigma_{\rm T}r_{\rm b}u_{\rm j}}{m_ec^2}$, where the subscript j takes the values 'B' (magnetic field), 'ex' (external photon field), 'syn' (synchrotron photons) and 'ssc,i' (i-th generation of SSC photons). The photon compactness can be also written as $\ell_\gamma=\frac{L_\gamma\sigma_{\rm T}}{4\pi r_{\rm b}m_ec^3}$, where L_γ is the photon luminosity.
- the injection compactness of electrons is given by $\ell_{\rm e}^{\rm inj}=\frac{\sigma_{\rm T}L_{\rm e}^{\rm inj}}{4\pi r_{\rm b}m_ec^3}=\frac{r_{\rm b}^2\sigma_{\rm T}Q_0\gamma_0}{3c}$.
- the ratio ξ of the cooling and escape timescales of electrons with Lorentz factor γ_0 is written as $\xi=\frac{3m_ec^2}{4\sigma_{\rm T}r_{\rm b}u_{\rm tot}\gamma_0}=\frac{3}{4\ell_{\rm tot}\gamma_0}$. If $\xi<1$, then electron cooling becomes important (fast cooling). Otherwise, electron cooling is negligible (slow cooling).
- the ratio of the external photon to the magnetic compactness is expressed through $f_{\rm ex}\equiv1+\frac{\ell_{\rm ex}}{\ell_B}$.

2. Results

Steady-state calculations: photon spectra

The parameter space of $f_{\rm ex}$ vs. $\ell_{\rm e}^{\rm inj}$ is shown in Fig. 1. The regions of fast and slow cooling are denoted with the letters "F" and "S", respectively. The abbreviation "CC" is used to mark the regions where the Compton catastrophe becomes relevant (for more details, see [4]). One can estimate the power-law index $\beta_{\rm cc}$ of the photon spectrum in the CC limit by assuming that the bolometric luminosity of each component is a good proxy for the peak luminosity and by using the approximate relation $\frac{L_{\rm ssc,i+1}^{\rm obs}}{L_{\rm ssc,i}^{\rm obs}}\approx\left(\frac{\epsilon_{\rm ssc,i+1}}{\epsilon_{\rm ssc,i}}\right)^{1-\beta_{\rm cc}}$ where $\epsilon_{\rm ssc,i}\simeq(4/3)^i b\gamma_0^{2(i+1)}m_ec^2$. The result is (see also [6, 4])

$$\beta_{\rm cc}\simeq\begin{cases}1-\frac{\log\left(4\ell_{\rm e}^{\rm inj}\gamma_0\right)}{\log\left(4\gamma_0^2/3\right)}, & \text{slow cooling}\\ 1-\frac{\log\left(3\ell_{\rm e}^{\rm inj}/\ell_B\right)}{(N_{\rm T}+1)\log\left(4\gamma_0^2/3\right)}, & \text{fast cooling}\end{cases}$$

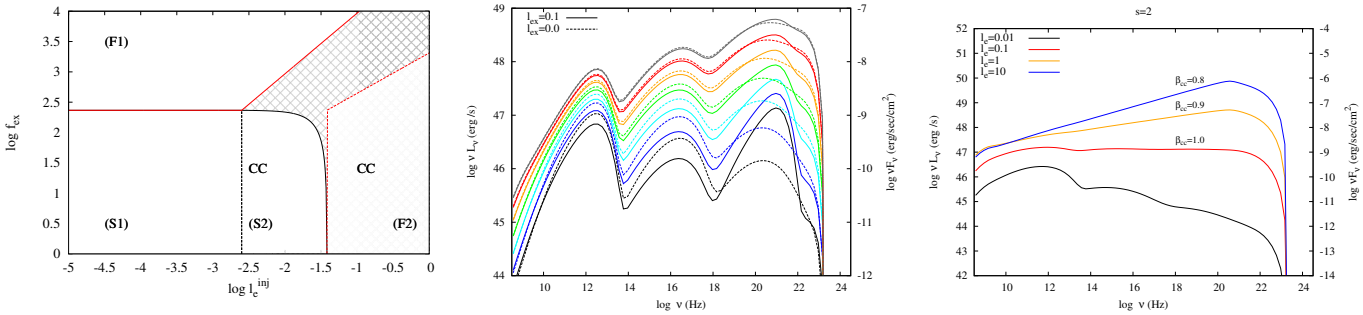

Figure 1: **Left panel:** Plot of $f_{\rm ex}$ vs. $\ell_{\rm e}^{\rm inj}$ for $\gamma_0 = 100$ and $\ell_B = 3 \times 10^{-5}$. For a fixed ℓ_B, the system may enter the fast cooling regime ($\xi < 1$) either for high values of $\ell_{\rm e}^{\rm inj}$ (lower right region) or high external photon compactnesses (upper left and middle regions). In the region F_1, the main channel of electron energy losses is synchrotron radiation and EC scattering. In fact, there is a transition from synchrotron to EC scattering cooling, as one moves towards higher values of $f_{\rm ex}$ within the F_1 region. In the F_2 region, electrons lose energy preferentially by the SSC process. Moreover, the energy density of higher order SSC photon generations becomes larger, and as such, it dominates the total energy density which appears in the electron cooling term. The regions S_1 and S_2 of the slow cooling regime ($\xi > 1$) occupy the lower left and middle part of the parameter space, where both the electron and external photon compactnesses are low/moderate. **Middle panel:** An example of steady-state MW spectra obtained for different values of $\ell_{\rm e}^{\rm inj}$, starting from 10^{-2} (black lines) and increasing up to $10^{-0.2}$ (grey lines) with logarithmic increments of 0.3. The MW spectra obtained for $\ell_{\rm ex} = 0$ are over-plotted with dashed lines. Other parameters used are $\gamma_0 = 100$, $B = 10$ G, $r_{\rm b} = 10^{16}$ cm, $\ell_B = 3 \times 10^{-2}$, $\ell_{\rm e}^{\rm inj} = 10^{-2}$, $\Gamma = 10$, $\epsilon_{\rm ex,\star} = 1$ eV, where $\epsilon_{\rm ex,\star} = 1$ is the characteristic energy of the external photon field . The flux values correspond to a source with a fiducial redshift $z = 0.2$. **Right panel:** Steady-state multi-wavelength photon spectra obtained for a power-law injection of electrons with index $s = 2$. Different types of lines correspond to the values of $\ell_{\rm e}^{\rm inj}$ marked on the plot.

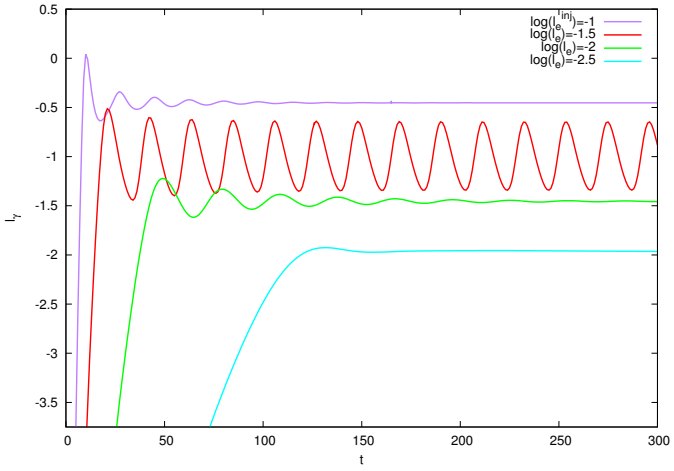

Figure 2: Photon light curve for different values of $\ell_{\rm e}^{\rm inj}$. Other parameters used are $R = 10^{14} cm$,$B = 0.1G$,$\gamma_{\rm max} = 10^{0.8}$. A necessary condition for the limit cycles to appear is a low value of $\gamma_{\rm max}$.

Time-dependent calculations: light curves

The numerical treatment of the problem allows us to augment the relativistic electron kinetic equation with more processes, such as pair injection due to photon-photon absorption, and to make use of the full expressions for the synchrotron and Compton emissivities in the relativistic limit. In addition, we write an accompanying equation for photons, which is coupled to the one for electrons. The numerical code is used is presented in [5], although some of its features have been improved since then.

Numerical calculations also allow for a time-dependent study of the problem. As an indicative example, we show in Fig. 2 the photon luminosity as a function of time for various $\ell_{\rm e}^{\rm inj}$ values. For low values of $\ell_{\rm e}^{\rm inj}$, the system reaches quickly a steady-state but for higher values of $\ell_{\rm e}^{\rm inj}$ it exhibits limit cycles (seemingly is like the behavior of [7]). Further analysis is required for determining the conditions that drive the system to an oscillatory state.

Acknowledgements: Support for this work was provided by NASA through Einstein Postdoctoral Fellowship grant number PF3 140113 awarded by the Chandra X-ray Center, which is op- erated by the Smithsonian Astrophysical Observatory for NASA under contract NAS8-03060 (MP) and by an ERC advanced grant GRBs, by the I-CORE Program of the Planning and Budgeting Committee and The Israel Science Foundation grant No 1829/12 and by ISA grant 3-10417 (TP).

[1] Readhead, A.C.S. *ApJ*, **426** (426), 51

[2] Tsang, O. & Kirk, J.G. *AAP*, **463** (2012), 145

[3] Longair M.S. *Cambridge, UK: Cambridge University Press*, (2011)

[4] Petropoulou, M., Piran, T. & Mastichiadis, A. *MNRAS*, **452** (2015), 3226-3245

[5] Mastichiadis, A. & Kirk, J.G. *AAP*, **295** (1995), 613

[6] Bjornsson, C.I.& Aslaksen, T. *ApJ*, **533**, (2000), 787

[7] Petropoulou, M. & Mastichiadis, A. *MNRAS*, **421** (2012), 2325-2341